Earthline Journal of Chemical Sciences
E-ISSN: 2581-9003; CODEN: EJCSB4
Volume 13, Number 3, August 2026, Pages 217-229
https://doi.org/10.34198/ejcs.13326.17.217229

Interaction of FOX-7 with aminonitroethylenes – A DFT treatment

Lemi Türker

Department of Chemistry, Middle East Technical University, Üniversiteler, Eskişehir Yolu No: 1, 06800 Çankaya/Ankara, Turkey
e-mail: lturker@gmail.com; lturker@metu.edu.tr

Abstract

Interaction of FOX-7 (a well known explosive), and *cis*, *trans* and *geminal* aminonitroethylenes are considered within the realm of density functional theory at the level of B3LYP/6-31++G(d,p). Both of the partners of the composites are pull-push systems. The collected data for the isomeric composites have revealed that the optimized structures of them have exothermic heats of formation and favorable Gibbs free energy of formation values. They are thermally favored and electronically stable at the standard states. Various structural and quantum chemical data have been collected and discussed, including IR and UV-VIS spectra. Some intra and inter hydrogen bonding possibilities exist in composites. The electrostatic interactions between the components are mainly charge-charge, dipole-dipole or both types. Mutual interactions of the partners affect their molecular orbital energies, interfrontier molecular orbital energy gaps etc., at different extents, thus dictate variations among the various properties of the composites.

1. Introduction

FOX-7 is a novel insensitive high-energy material exhibiting good thermal stability and low sensitivity. In addition to that, it possesses excellent application performance among the solid propellants and insensitive ammunitions. It exhibits abundant chemical reactivity [1,2]. Also FOX-7 is much less sensitive than RDX explosive in terms of impact, friction, and electrostatic discharge sensitivities.

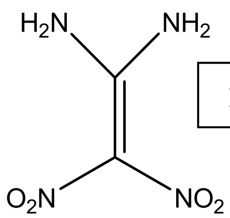

FOX-7

FOX-7 is classified as a push-pull type alkene having two electron-donating substituents (NH_2) on one end of C=C double bond and with two electron-accepting substituents (NO_2) at the other end [3,4]. This push-pull effect has decisive influence on both the dynamic behavior and the chemical reactivity of this class of compounds [3].

On the other hand, monoaminomononitroethylenes in the form of *cis*, *trans* and *geminal* (constitutional isomers) isomers have different extents of push-pull resonance effects which dictate various structural and potential properties [5]. Amino and nitro groups have donor and acceptor properties, respectively in terms of classical resonance theory. When they are attached to a double or a triple bond, a polar system may arise depending on the positions of the donor and acceptor groups.

Received: April 10, 2026; Accepted: May 15, 2026; Published online: May 20, 2026

Keywords and phrases: FOX-7, aminonitroethylenes, explosives, DFT calculations, pull-push.

Through the decades various scientists have investigated different aspects of push-pull effect on molecular behavior in terms of structure-activity relationships [6-16].

The present treatise considers the interaction of FOX-7 with aminonitroethylenes within the realm of density functional theory (DFT).

2. Method of Calculations

In the present study, all the initial optimizations of the structures leading to energy minima have been achieved first by using MM2 method which is then followed by semi empirical PM3 self consistent fields molecular orbital method [17-19]. Afterwards, the structure optimizations have been achieved within the framework of Hartree-Fock and finally by using density functional theory (DFT) at the level of B3LYP/6-31++G(d,p) [20,21]. Note that the exchange term of B3LYP consists of hybrid Hartree-Fock and local spin density (LSD) exchange functions with Becke's gradient correlation to LSD exchange [22]. The correlation term of B3LYP consists of the Vosko, Wilk, Nusair (VWN3) local correlation functional [23] and Lee, Yang, Parr (LYP) correlation correction functional [24]. In the present study, the normal mode analysis for each structure yielded no imaginary frequencies for the $3N\text{–}6$ vibrational degrees of freedom, where N is the number of atoms in the system. This search has indicated that the structure of each molecule considered corresponds to at least a local minimum on the potential energy surface. Furthermore, all the bond lengths have been thoroughly searched in order to find out whether any bond cleavages occurred or not during the geometry optimization process. All these computations were performed by using SPARTAN 06 program [25].

3. Results and Discussion

Figure 1 shows the optimized structures of the composites considered (they are some sort of isomers having bruto formula of $C_2H_4N_2O_2.C_2H_4N_4O_4$) as well as the direction of the dipole moment vectors of them. The figure

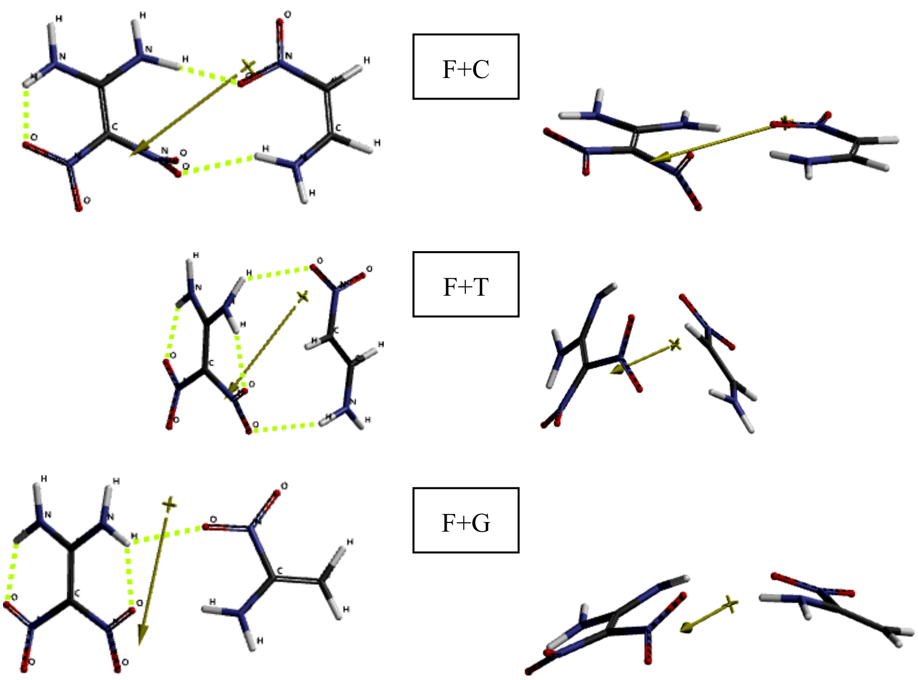

Figure 1. Optimized structures of the composites considered (two different views).

also displays the possible intra and inter molecular hydrogen bonding sites of the components. In the figure letter F stands for FOX-7 structure (1,1-diamino-2,2-dinitroethylene) whereas C, T and G stand for *cis*, *trans* and *geminal* aminonitroethylenes (ANEs), respectively.

Table 1 contains some thermo chemical properties of the composites considered. Whereas, Table 2 includes some energies of them. The data in Table 1 reveal that the standard heat of formation (H^o) values of the isomers are exothermic and they are favored according to their G^o (Gibbs free energy of formation) values. The algebraic order of H^o and G^o values are same as F+C< F+T< F+G, namely F+C has more exothermic H^o value than the others. Whereas S^o values follow the order of F+G> F+T> F+C.

Table 1. Some thermo chemical properties of the composites considered.

Composite	H^o	S^o (J/mol^o)	G^o
F+C	-2459274.626	478.26	-2459417.219
F+T	-2459264.486	480.46	-2459407.738
F+G	-2459233.266	480.50	-2459376.526

Energies in kJ/mol.

The data in Table 2 reveal that they are all electronically stable structures. The stability order is F+C> F+T> F+G. Thus, composite F+G represents the least stable composite among the all. Note that E, ZPE and E_C stand for the total electronic energy, zero point vibrational energy and the corrected total electronic energy, respectively [25]. Probably favorable steric factors and the hydrogen bondings possible between the donor and acceptor groups make composite F+C more stable than the others. In general attractive and repulsive forces are operative between the components of the composites and dictate the stability order in great extent.

Table 2. Some energies of the composites considered.

Composite	E	ZPE	E_C
F+C	-2459727.35	437.22	-2459290.13
F+T	-2459717.29	436.98	-2459280.31
F+G	-2459681.33	432.04	-2459249.29

Energies in kJ/mol.

Figure 2 displays the calculated bond lengths of the composites. Note the C-C bond lengths in FOX-7 and accompanying amino nitro ethylene partner in F+C, F+T and F+G. They are 1.41 Å and 1.37 Å; 1.43 Å and 1.36 Å; 1.43 Å and 1.34 Å, respectively. Also, C-NH_2 and C-NO_2 bond lengths subject to variations. All these show how pull-push effect in the composites changes as an intricate function of topology of the components. It is noteworthy that components affect each other in the composite form electrostatically and their apt of hydrogen bonding contributes additionally.

Figure 3 displays the electrostatic potential (ESP) maps of the composites considered where negative potential regions reside on red/reddish and positive ones on blue/bluish parts of the maps. In the case of composite F+C, amino groups of FOX-7 and *cis* amino nitroethylene component reside in blue/bluish part of the potential map. The nitro groups are in the reddish/yellowish region. However, those regions in FOX-7 possess much lower potential value than the respective value of the aminonitroethylene component. The situation in the case of F+T composite is quite different. The negative potential region of the *trans* aminonitroethylene component is more pronounced (where the nitro group resides). Note that the potential values on the amino and nitro groups in the composites are the resultant sum of contributions of the overlapped fields. The patches of positive and negative potential regions arise not only due to pure resonance effect (due to π-electron topology of the individual components) but also the hydrogen bondings between the components which perturb the whole π-electron topology of the composites. Electrostatic potential map of composite F+G is constructed within the influence of more complicated factors such that pull- push effect is somewhat veiled compared to the other cases.

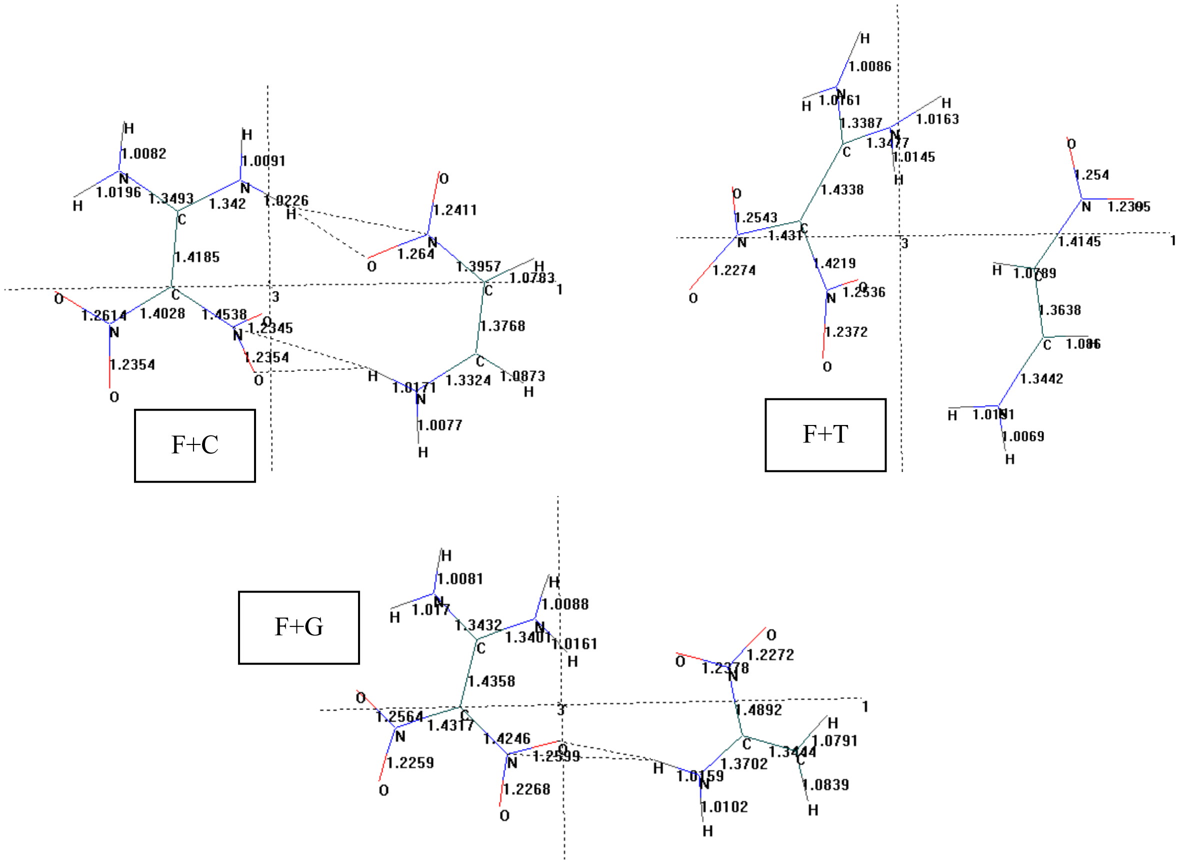

Figure 2. The calculated bond lengths of the composites (on axes of inertia).

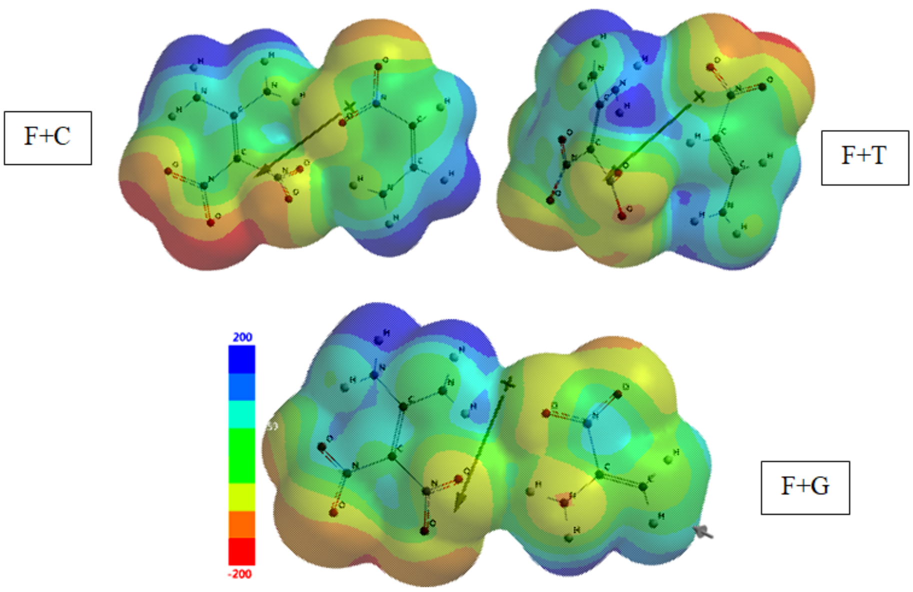

Figure 3. Electrostatic potential maps of the composites considered.

Figure 4 shows the chemical function descriptors (CFD's) of the composites considered Note that CFDs are attributes given to a molecule in order to characterize or anticipate its chemical behavior. In the figure different colors stand for different descriptors (Green: HBA; Purple: HBA, HBD and +ionizable). Note that HBA and HBD mean hydrogen bond acceptors and donors, respectively.

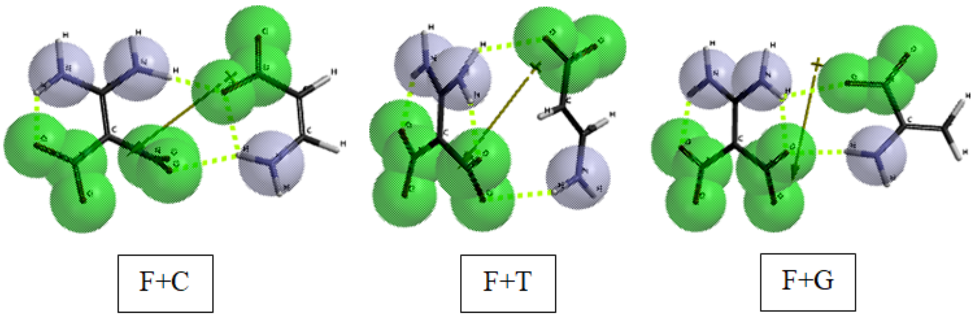

Figure 4. CFD's of the composites considered (Green: HBA; Purple: HBA, HBD and +ionizable).

All of the composites (indeed they are some sort of isomers) have the same number of the same kind of CFDs. Therefore, differences in properties of them should arise from the minor differences in the gross and fine topologies of the structures. It is noteworthy that the CFDs give an idea in designing molecular structure for some special purpose in structure-activity relationships such as Log P values, etc. (see below).

Figure 5 shows the electrostatic potential (ESP) charges on atoms of the composites considered. It is note worthy that the ESP charges are obtained by the program which uses a numerical method that generates charges, thus reproducing the electrostatic potential field from the entire wavefunction [25]. As seen in the figure, some intra and inter hydrogen bondings are possible in the composites. The over all group charges can give some idea about the direction and magnitude of the pull-push effect. The dipole moment vector in the case of F+C and F+T type composites originate from somewhere nearby the aminonitroethylene component and aims at the FOX-7 structure.

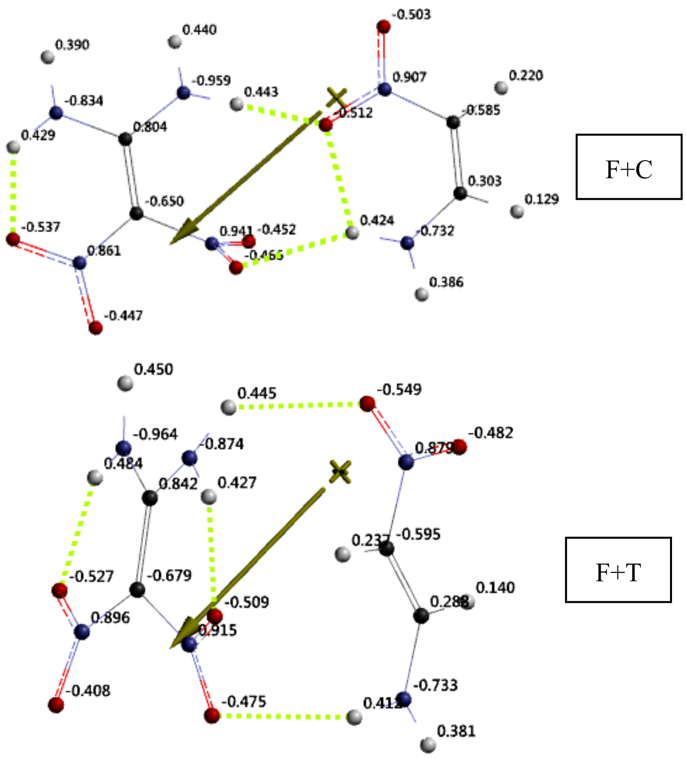

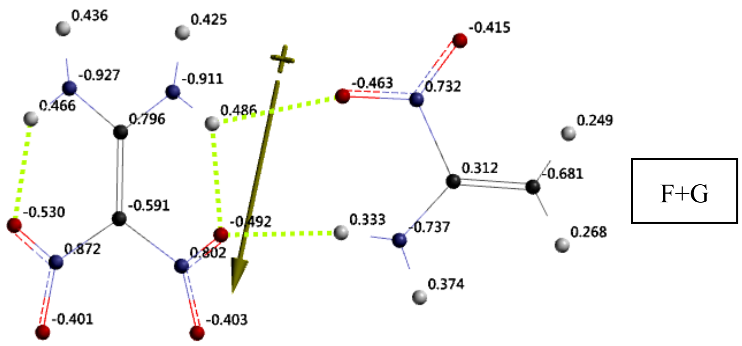

Figure 5. The ESP charges on atoms of the composites.

Table 3 shows some properties of the composites of interest. The polarizability is defined according to the formula [25].

Table 3. Some properties of the composites of interest.

Composites	Dipole moment	Polarizability	Cv (J/mol°)	Area (Å²)	Volume (Å³)	PSA (Å²)	Ovality
F+C	5.49	55.68	177.09	235.25	188.52	169.035	1.48
F+T	1.12	55.78	177.09	237.26	189.03	172.911	1.49
F+G	4.66	55.83	181.77	236.91	188.74	170.010	1.49

Dipole moments in debye units. Polarizabilities in 10^{-30} m^3 units.

$$\text{Polarizability} = 0.08{*}V - 13.0353{*}h + 0.979920{*}\, h^2 + 41.3791$$

where V and h are the Van der Waals volume and hardness, respectively. Hardness is defined as,

$$\text{Hardness} = -(\varepsilon_{HOMO} - \varepsilon_{LUMO})/2$$

where ε_{HOMO} and ε_{LUMO} are energies of the highest occupied and lowest unoccupied molecular orbital levels.

Polar surface area (PSA) is defined as the amount of molecular surface area arising from polar atoms (N,O) together with their attached hydrogen atoms. It is claimed that molecules with PSA values greater than 140 Å² tend to be poor at permeating cell membranes whereas to penetrate the blood-brain barrier a PSA value of a molecule should be less than 90 Å² [26,27].

The Cv values of F+C and F+T are the same but the respective value of F+G is higher than the others.

Some further properties of the composites of interest are displayed in Table 4. The log P values of composites F+C and F+T are some small negative figures whereas the respective value of F+G is also small but a positive value.

Solvation energy is the total energy change that occurs when solute particles are surrounded by and interact with solvent molecules, transferring them from a vacuum or gas phase into a liquid solvent [4]. It measures the stability of a solute within a solvent, representing the strength of solvent-solute interactions. Note that a negative solvation energy indicates an exothermic process, which increases the stability of the solution. The algebraic order of the solvation energies is F+C< F+G< F+T.

Table 4. Some further properties of the composites of interest.

Composite	Eaq	Log P	Solvation E
F+C	-2459836.51	-0.54	-109.16
F+T	-2459780.79	-0.54	-63.51
F+G	-2459766.35	0.08	-85.02

Energies in kJ/mol.

Partition coefficients are important property and useful in estimating the distribution of molecules between different solvent systems. Hydrophobic molecules with high octanol-water partition coefficients are mainly distributed to hydrophobic areas such as lipid bilayers of cells. Conversely, hydrophilic ones (low octanol/water partition coefficients) are found primarily in aqueous regions such as blood serum.

Figure 6 displays the calculated IR spectra of the composites considered. The spectrum of F+C has two relatively small peaks at 3700 cm^{-1} and 3681 cm^{-1} which are N-H stretchings of FOX-7 component. The peak at 3512 cm^{-1} is the N-H stretchings of *cis* aminonitroethylene. The hydrogen bonded N-H stretching of FOX-7 occurs at 3380 cm^{-1} as a strong peak. The scissoring modes of FOX-7 N-H happen at 1718-1646 cm^{-1}. The C-NO_2 stretch is strong and appears at 1315 cm^{-1}.

The spectrum of F+T possesses asymmetrical N-H stretchings of FOX-7 and *trans* aminonitroethylene components at 3711 cm^{-1} and 3693 cm^{-1}, respectively. The hydrogen bonded N-H stretchings (asym.) of FOX-7 and aminonitroethylene occur at 3617 cm^{-1} and 3540 cm^{-1}, respectively. Whereas symmetrical N-H stretchings of FOX-7 take place at 3510 cm^{-1}. Various bendings happen in between 1708 cm^{-1} and 1532 cm^{-1}. The peaks at 1394 cm^{-1} and 1297 cm^{-1} stand for some skeletal motions of aminonitroethylene component.

As for the spectrum of F+G component, the peaks at 3696 cm^{-1} and 3692 cm^{-1} belong to asymmetrical N-H stretchings of FOX-7 component, followed by asymmetrical N-H stretching of aminonitroethylene at 3674 cm^{-1}. The peak at 3531 cm^{-1} is the symmetrical N-H stretch of aminonitroethylene component. The symmetrical intra molecular hydrogen bonded N-H stretch of FOX-7 component occurs at 3475 cm^{-1}. Carbon-carbon stretching occurs at 1725 cm^{-1} as a weak peak. The region of 1651-1634 cm^{-1} possesses various bendings.

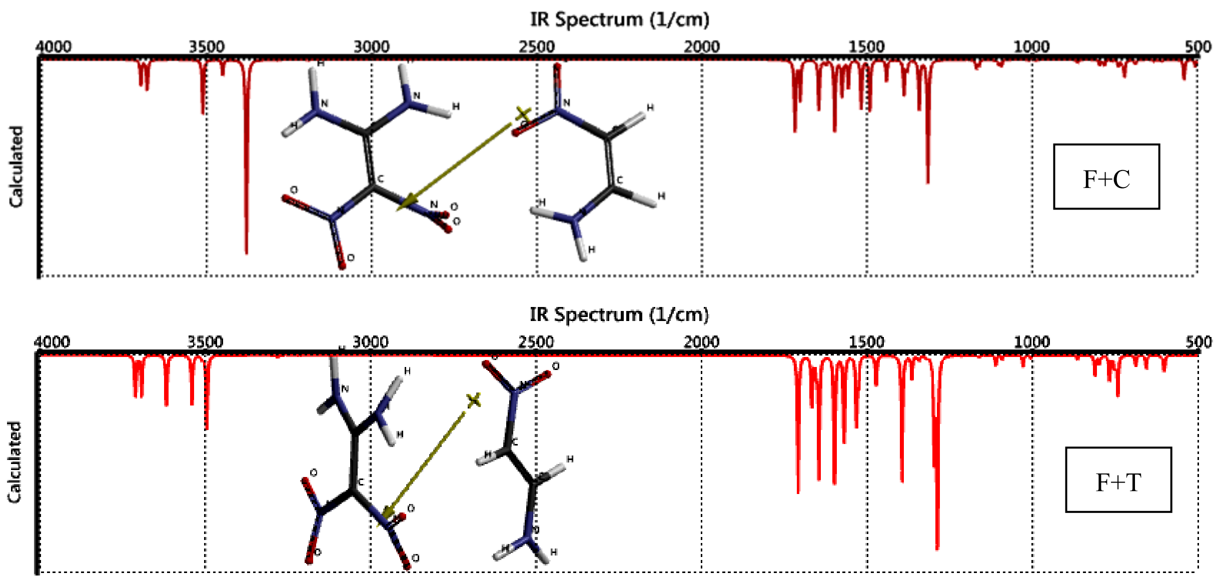

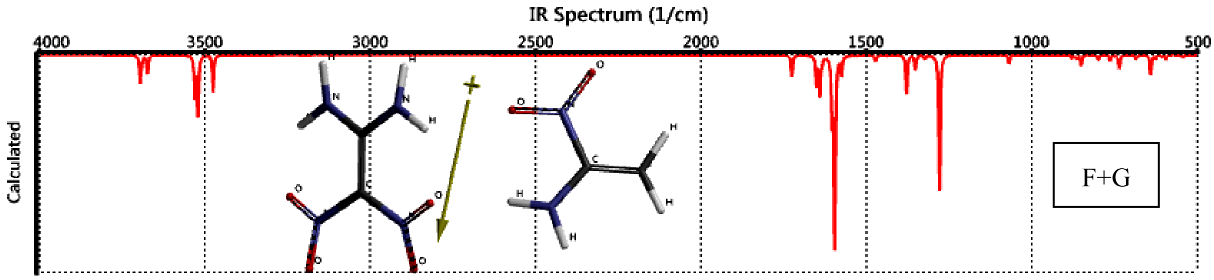

Figure 6. Calculated IR spectra of the composites considered.

Figure 7 shows the local ionization maps of the composites considered, where conventionally red/reddish regions (if any exists) on the density surface indicate areas from which electron removal is relatively easy, meaning that they are subject to electrophilic attack. Note that the local ionization potential map is a graph of the value of the local ionization potential on an isodensity surface corresponding to a van der Waals surface.

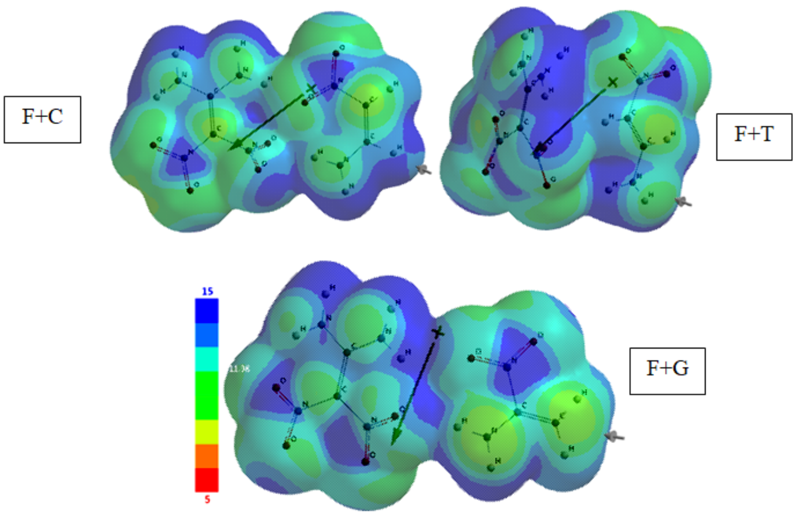

Figure 6. Local ionization maps of the composites considered.

Figure 7 shows the LUMO maps of the isomers considered. A LUMO map displays the absolute value of the LUMO on the electron density surface. The blue color stands for the maximum value of the LUMO and the color red, the minimum value.

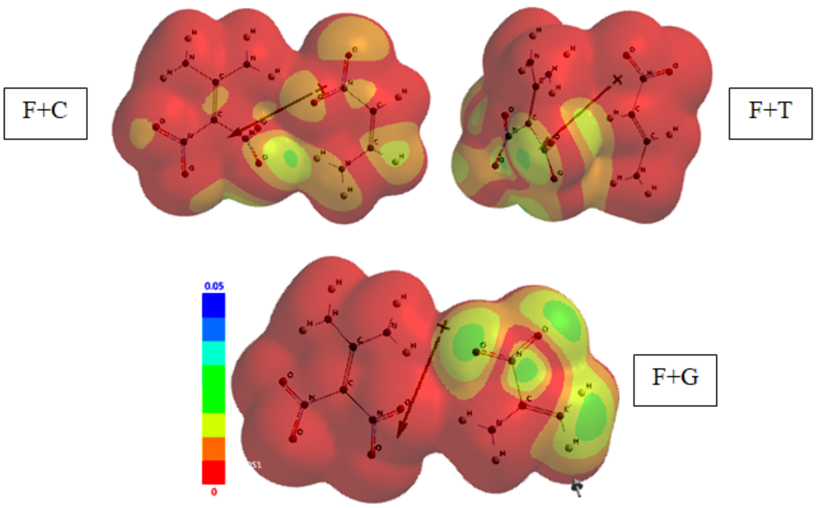

Figure 7. The LUMO maps of the composites considered.

Figure 8 shows the bond densities of the composites considered. The bond density contains fewer electrons in total and demarks atomic connectivity. The figure clearly indicates that in each case there is no bond density between the components of the composite. However, in each component bond density varies depending on the pull-push power of the groups (namely amino and nitro groups), configuration and conformation of the substituents etc.

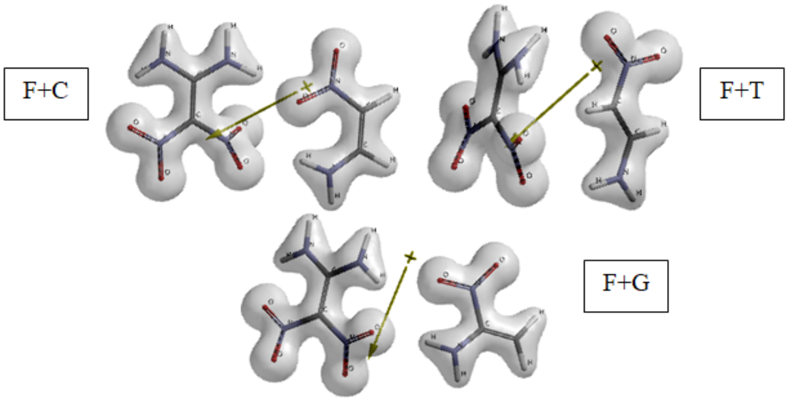

Figure 8. Bond densities of the composites considered.

Figure 9 displays some of the molecular orbital energy levels of the composites. As seen in the figure the energy difference between the HOMO and NEXTHOMO levels increase gradually going from F+C to F+G. On the other hand, composite F+G is characterized with the smallest LUMO-NEXTLUMO energy level difference (energy gap). Since in each composite one of the components is the same, FOX-7, all the variations seems to be due to the presence of the other component, namely variants of aminonitroethylene. However, one should not over neglect that the apparent outcome is the result of mutual interaction of the components. The electrostatic interactions, as an intricate manner shuffle the orbital energies, affect the dipole-dipole interactions, etc.

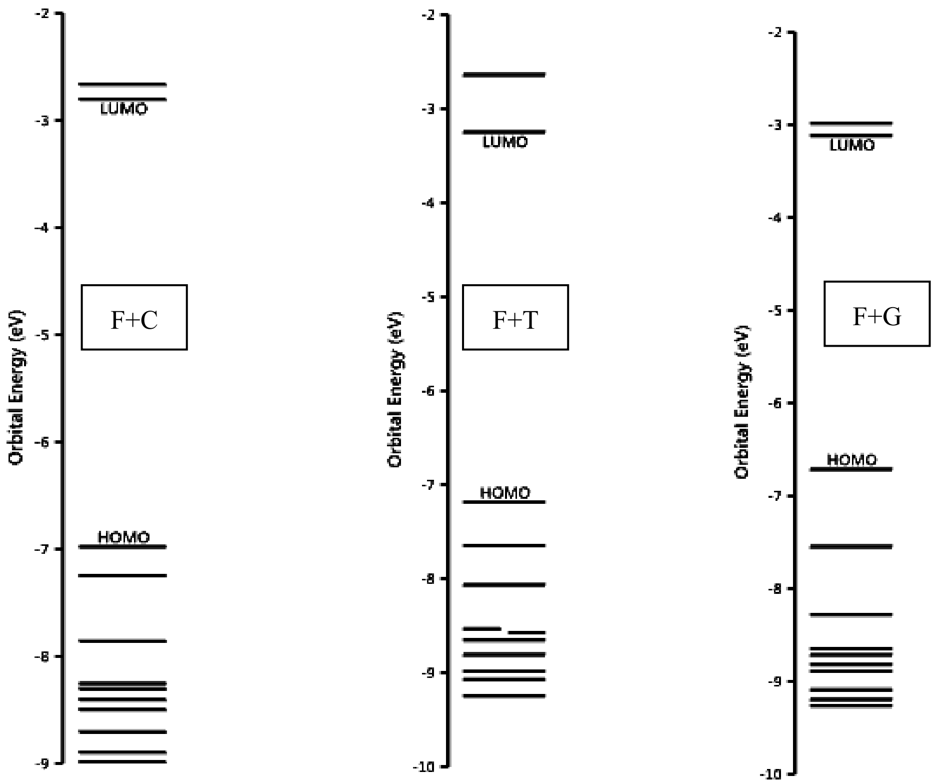

Figure 9. Some of the molecular orbital energy levels of the composites.

Table 5 lists the HOMO, LUMO energies and interfrontier molecular orbital energy gap, Δε, ($\Delta\varepsilon = \varepsilon_{LUMO} - \varepsilon_{HOMO}$) values of the composites considered. The HOMO and LUMO energies follow algebraic order of F+T< F+C< F+G and F+T< F+G< F+C, respectively. Consequently, the order of Δε values fall in to the sequence of F+G< F+T< F+C.

Table 5. The HOMO, LUMO energies and Δε values of the composites considered.

Composite	HOMO	LUMO	Δε
F+C	-673.21	-270.47	402.74
F+T	-693.26	-313.66	379.6
F+G	-647.50	-300.66	346.84

Energies in kJ/mol.

The configuration and conformation of the donor and acceptor groups in the components of the composites highly affect the extended conjugation which is responsible for the HOMO-LUMO energy separation. On the other hand, any composite having any ballistic property which correlates with the narrowness of the HOMO-LUMO energy separation should have the highest value between the composites (isomers) considered. An example is the impact sensitivity, that is narrower the gap, the explosive becomes more sensitive to an impact stimulus [28,29]. In the present case, composite F+G should be characterized with the highest and F+C the lowest impact sensitivity.

Figure 10 shows the HOMO and LUMO patterns of the composites considered. As seen in the figure generally π-symmetry exists. In the case of composite F+C, aminonitroethylene does not contribute into the LUMO level at all. Whereas in F+T, this time FOX-7 has quite negligible contribution of ethylenic carbon having the nitro groups. Whereas the LUMO does not have any contribution from the *trans* aminonitroethylene component.

As for the composite F+G, again FOX-7 component does not contribute to the HOMO level.

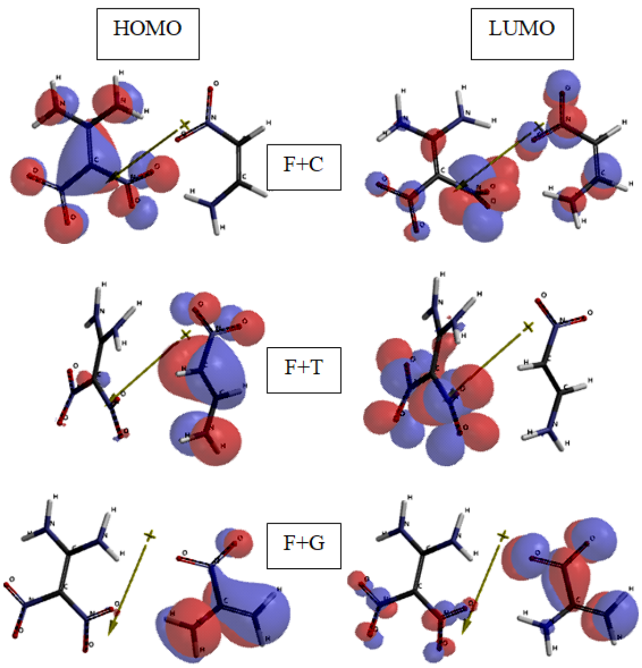

Figure 10. The HOMO and LUMO patterns of the composites considered.

Figure 11 displays the calculated UV-VIS (time dependent density functional, TDDFT) spectra of the composites. In all the composites the spectra spread over both the UV and VIS parts of the spectrum. Although, in the case of F+C the two peaks are distinct (316.32 nm and 392.61 nm.), in the other composites they appear as shoulder which is at 350.45 nm., in F+T and accompanies the main peak at 312.53 nm, and in F+G composite, the shoulder at 314.18 nm accompanies the main peak at 379.61 nm.

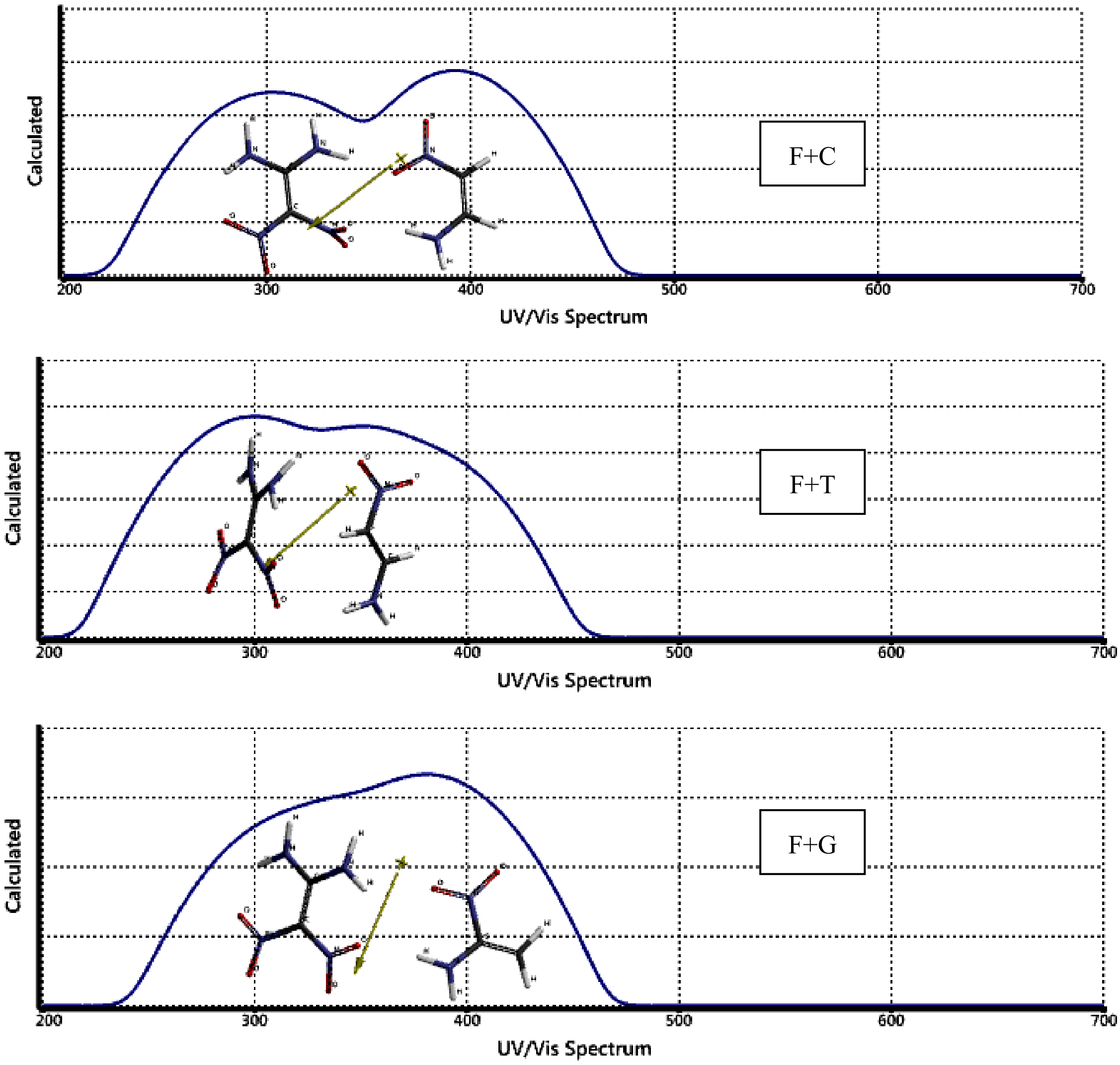

Figure 11. Calculated UV-VIS spectra of the composites considered.

It is to note worthy that intensities of the peaks are related to magnitudes of the transition moments between the orbitals involved which vary from structure to structure [30-32].

4. Conclusion

In the present DFT treatment, the interaction of FOX-7 with aminonitroethylenes are considered within the restrictions of the density functional theory, at the level of B3LYP/6-31++G(d,p). The results reveal that all the FOX-7+ ANE composites have exothermic heat of formation values and favorable Gibbs free energy of formation values in vacuum conditions. All the composites considered are electronically stable. The components electrostatically interact with each other, thus induced intermolecular push-pull effect occurs which affects the intra and inter hydrogen bonding possibilities, and shuffles molecular orbital energies. Thus, various properties of the components might be different in the composite form. Hence, a kind of property tuning could be achieved in order to vary the properties of the composites which might have some desirable properties.

References

[1] Zhang, Y., Sun, Q., Xu, K., Song, J., & Zhao, F. (2016). Review on the reactivity of 1,1-diamino-2,2-dinitroethylene (FOX-7). *Propellants, Explosives, Pyrotechnics, 41*, 35–52. https://doi.org/10.1002/prep.201500065

[2] Baum, K., Nguyen, N. V., Gilardi, R., Flippen-Anderson, J. L., & George, C. (1992). Nitration of 1,1-diamino-2,2-dinitroethylenes. *Journal of Organic Chemistry, 57*, 3026–3030. https://doi.org/10.1021/jo00037a015

[3] Kleinpeter, E. (2006). Push-pull alkenes: Structure and π-electron distribution. *Journal of the Serbian Chemical Society, 71*(1), 1–17. https://doi.org/10.2298/JSC0601001K

[4] Anslyn, E. V., & Dougherty, D. A. (2006). *Modern physical organic chemistry*. University Science Books.

[5] Türker, L. (2025). Some aminonitroethylenes and their interactions with each other – A DFT treatment. *Earthline Journal of Chemical Sciences, 12*(3), 239–256. https://doi.org/10.34198/ejcs.12325.239256

[6] Yanai, H., Suzuki, T., Kleemiss, F., Fukaya, H., Malaspina, L. A., Grabowsky, S., & Matsumoto, T. (2019). Chemical bonding in polarized push-pull ethylenes. *Angewandte Chemie International Edition, 58*(26), 8839–8844. https://doi.org/10.1002/anie.201904176

[7] Shainyan, B. A., Fettke, A., & Kleinpeter, E. (2008). Push-pull vs captodative aromaticity. *Journal of Physical Chemistry A, 112*(43), 10895–10903. https://doi.org/10.1021/jp804999m

[8] Pappalardo, R. R., Marcos, E. S., Ruiz-López, M. F., & Rinaldi, D. (1991). Theoretical study of simple push-pull ethylenes in solution. *Journal of Physical Organic Chemistry, 4*(3), 141–148. https://doi.org/10.1002/poc.610040304

[9] Politzer, P., Concha, M. C., Grice, M. E., Murray, J. S., Lane, P., & Habibollazadeh, D. (1998). Computational investigation of the structures and relative stabilities of amino/nitro derivatives of ethylene. *Journal of Molecular Structure: THEOCHEM, 452*, 75–83. https://doi.org/10.1016/S0166-1280(98)00136-5

[10] Kleinpeter, E., Klod, S., & Rudorf, W.-D. (2004). Electronic state of push-pull alkenes: An experimental dynamic NMR and theoretical ab initio MO study. *Journal of Organic Chemistry, 69*(13), 4317–4329. https://doi.org/10.1021/jo0496345

[11] Ababneh-Khasawneh, M., Fortier-McGill, B. E., Occhionorelli, M. E., & Bain, A. D. (2011). Solvent effects on chemical exchange in a push-pull ethylene as studied by NMR and electronic structure calculations. *Journal of Physical Chemistry A, 115*(26), 7531–7537. https://doi.org/10.1021/jp201885q

[12] Türker, L., Bayar, Ç. Ç., & Balaban, A. T. (2010). A DFT study on push-pull (aminonitro) fulminenes and hexahelicenes. *Polycyclic Aromatic Compounds, 30*(2), 91–111. https://doi.org/10.1080/10406631003756005

[13] Türker, L., & Bayar, Ç. Ç. (2010). A DFT study on disubstituted R-hexahelicenes having donor/acceptor groups. *Procedia Computer Science, 1*(1), 1155–1164. https://doi.org/10.1016/j.procs.2010.04.129

[14] Türker, L. (2025). Some dinitramines from tetraaminoethylene and their interactions with magnesium – DFT study. *Earthline Journal of Chemical Sciences, 12*(2), 193–205. https://doi.org/10.34198/ejcs.12225.193205

[15] Türker, L. (2025). Charged forms of aminonitroethylene isomers – A DFT study. *Earthline Journal of Chemical Sciences, 12*(4), 397–407. https://doi.org/10.34198/ejcs.12425.397407

[16] Türker, L. (2026). Push-pull interactions in cis/trans diaminodinitro ethylenes – DFT treatment. *Earthline Journal of Chemical Sciences, 13*(1), 1–12. https://doi.org/10.34198/ejcs.13126.01.001012

[17] Stewart, J. J. P. (1989). Optimization of parameters for semi-empirical methods I. *Journal of Computational Chemistry, 10*, 209–220. https://doi.org/10.1002/jcc.540100208

[18] Stewart, J. J. P. (1989). Optimization of parameters for semi-empirical methods II. *Journal of Computational Chemistry, 10*, 221–264. https://doi.org/10.1002/jcc.540100209

[19] Leach, A. R. (1997). *Molecular modeling*. Longman.

[20] Kohn, W., & Sham, L. J. (1965). Self-consistent equations including exchange and correlation effects. *Physical Review, 140*, A1133–A1138. https://doi.org/10.1103/PhysRev.140.A1133

[21] Parr, R. G., & Yang, W. (1989). *Density functional theory of atoms and molecules*. Oxford University Press.

[22] Becke, A. D. (1988). Density-functional exchange-energy approximation with correct asymptotic behavior. *Physical Review A, 38*, 3098–3100. https://doi.org/10.1103/PhysRevA.38.3098

[23] Vosko, S. H., Wilk, L., & Nusair, M. (1980). Accurate spin-dependent electron liquid correlation energies for local spin density calculations: A critical analysis. *Canadian Journal of Physics, 58*, 1200–1211. https://doi.org/10.1139/p80-159

[24] Lee, C., Yang, W., & Parr, R. G. (1988). Development of the Colle-Salvetti correlation energy formula into a functional of the electron density. *Physical Review B, 37*, 785–789. https://doi.org/10.1103/PhysRevB.37.785

[25] SPARTAN 06. (2006). Wavefunction Inc.

[26] Hitchcock, S. A., & Pennington, L. D. (2006). Structure-brain exposure relationships. *Journal of Medicinal Chemistry, 49*(26), 7559–7583. https://doi.org/10.1021/jm060642i

[27] Shityakov, S., Neuhaus, W., Dandekar, T., & Förster, C. (2013). Analysing molecular polar surface descriptors to predict blood-brain barrier permeation. *International Journal of Computational Biology and Drug Design, 6*(1–2), 146–156. https://doi.org/10.1504/IJCBDD.2013.052195

[28] Anbu, V., Vijayalakshmi, K. A., Karunathan, R., Stephen, A. D., & Nidhin, P. V. (2019). Explosive properties of high energetic trinitrophenyl nitramide molecules: A DFT and AIM analysis. *Arabian Journal of Chemistry, 12*(5), 621–632. https://doi.org/10.1016/j.arabjc.2016.09.023

[29] Badders, N. R., Wei, C., Aldeeb, A. A., Rogers, W. J., & Mannan, M. S. (2006). Predicting the impact sensitivities of polynitro compounds using quantum chemical descriptors. *Journal of Energetic Materials, 24*, 17–33. https://doi.org/10.1080/07370650500374326

[30] Turro, N. J. (1991). *Modern molecular photochemistry*. University Science Books.

[31] Barrow, G. M. (1962). *Introduction to molecular spectroscopy*. Kogakusha.

[32] Harris, D. C., & Bertolucci, M. D. (1978). *Symmetry and spectroscopy*. Oxford University Press.